Journal Name

Dynamic Article Links ►

Cite this: DOI: 10.1039/c0xx00000x

www.rsc.org/xxxxxx

ARTICLE TYPE

Competitive formation of both long-range 5′– 5′and short-range antiparallel 3′– 3′ DNA interstrand cross-links by a trinuclear platinum complex on binding to a 10-mer duplex

Rasha A. Ruhayel,[a,c] Susan J. Berners-Price*[a,c] and Nicholas P. Farrell*[b,a]

Received (in XXX, XXX) Xth XXXXXXXXX 200X, Accepted Xth XXXXXXXXX 200X
DOI: 10.1039/b000000x

2D [^{1}H, ^{15}N] HSQC NMR spectroscopy has been used to monitor the reaction of fully ^{15}N-labelled [{*trans*-PtCl(NH$_3$)$_2$}$_2$(μ-*trans*-Pt(NH$_3$)$_2${NH$_2$(CH$_2$)$_6$NH$_2$}$_2$)]$^{4+}$ (Triplatin, BBR3464 or 1,0,1/*t*,*t*,*t* (^{15}N-**1**)) with the self-complementary 10-mer DNA duplex 5′-{d(ACGTATACGT)$_2$} (duplex **I**) at pH 5.4 and 298 K. Initial electrostatic interactions were observed in the minor groove of the duplex, followed directly by aquation to form the monoaqua monochloro species. There was evidence for two discrete monofunctional adducts, through covalent binding at the guanine N7 sites, and one had distinctly different ^{1}H/^{15}N chemical shifts to those observed previously in analogous reactions. Bifunctional adduct formation followed by binding at a second guanine N7 site with evidence for both the 3′-3′ 1,2-GG and 5′-5′ 1,6-GG interstrand cross-links in a ratio of 2:1. The results show that cross-link preference is kinetically controlled and will depend critically on the reaction conditions, explaining why in a previous reaction of **1** with duplex **I** the major adduct isolated by HPLC had two simultaneous 3′–3′ 1,2-interstrand cross-links.

Introduction

The polynuclear platinum complex (PPC) chemotype is structurally distinct from mononuclear cisplatin and is exemplified by the archetypal dinuclear [{*trans*-PtCl(NH$_3$)$_2$}$_2$(μ-NH$_2$(CH$_2$)$_6$NH$_2$)]$^{2+}$ (BBR3005 or 1,1/*t*,*t*) and trinuclear [{*trans*-PtCl(NH$_3$)$_2$}$_2$(μ-*trans*-Pt(NH$_3$)$_2${NH$_2$(CH$_2$)$_6$NH$_2$}$_2$)]$^{4+}$ (Triplatin, BBR3464 (**1**) or 1,0,1/*t*,*t*,*t*) (Chart 1). Triplatin advanced to Phase II human clinical trials and remains proof of concept for the utility of "non-classical" structures as anti-cancer agents.[1] The development has been predominantly predicated on production of DNA lesions structurally distinct from those formed by cisplatin and congeners.[2] Especially the formation of long-range interstrand and intrastrand cross-links produces a DNA binding profile distinct from the mononuclear-based agents and, indeed, unlike those of any agent in clinical use. Complementary molecular biology and spectroscopic approaches have examined the structures and kinetics of formation of these adducts.[2-6] Overall, the results support the view that the cytotoxicity of Triplatin may arise from the sum of the contributions of the multiple DNA cross-links available to this PPC.[2]

A significant aspect of this research has been the description of non-interconvertible *directional isomers* of long-range interstrand cross-links (IXLs). Cross-links occur not only in the ''normal'' 5′–5′ direction, since DNA is normally read from the 5′–side, but also in the ''opposite'' antiparallel 3′–3′ direction.[7] The directionality of cross-link formation is dictated by the length of the cross-link. The 1,2-IXL forms in only the 3′–3′ direction; the 1,4-IXL forms in both directions (in approximately equal proportions) while the 1,6-IXL forms in only the 5′–5′ direction.[7] Further, the presence of a charged linker (as in Triplatin) enhances directional isomer formation in the 1,4-IXL, whereas the simple dinuclear compound with the hexanediamine linker (1,1/*t*,*t*, Chart 1) forms in only the 5′–5′ direction.[6, 7] To our knowledge, this is the only example of anti-cancer drugs behaving in this manner.[8, 9]

We have previously studied the mechanism and kinetics (where possible) of 1,6-GG and/or 1,4-GG (5′–5′ and 3′–3′) cross-links using 2D [^{1}H,^{15}N] NMR spectroscopy on defined sequence-specific oligonucelotides for a variety of PPCs.[4-6, 10-12] In the case of Triplatin, whilst only one conformer was observed for the 5′–5′ 1,6–GG interstrand cross-link, two discrete conformers were observed for the 5′–5′ 1,4–GG cross-link. In contrast, NMR studies on the formation of the 3′–3′ isomer of the 1,4–GG cross-link showed that it is most likely highly distorting compared to the 5′–5′ counterpart.[6] Using larger sequences, differential scanning calorimetry, chemical probes, and use of the minor groove binder Hoechst 33258 as probe, showed that both cross-links occur as a pair of conformers and that all four conformers affect DNA in a distinctly different way.[13]

The short-range cross-link, 1,2–GG, is of interest as it forms exclusively in the 3′–3′ direction.[7] Reaction of Triplatin with the DNA duplex 5′–{d(ACGTATACGT)$_2$} (duplex **I**, Chart 1)

[a]*Institute for Glycomics, Griffith University, Gold Coast Campus, QLD 4222, Australia. Tel: +61 7 3735 7290, E-mail: s.berners-price@griffith.edu.au*
[b]*Department of Chemistry, Virginia Commonwealth University Richmond, Virginia, 23284-2006 USA. E-mail: npfarrell@vcu.edu.au*
[c]*School of Chemistry and Biochemistry, University of Western Australia, 35 Stirling Highway, Crawley, WA 6009, Australia*

resulted in formation of two simultaneous 3′–3′ 1,2–GG IXLs.[14] The structure as analyzed by 2D NMR spectroscopy (NOESY, COSY, TOCSY) is quite distinct from the analogous cisplatin 1,2-interstrand $(GC)_2$ adduct where the cytosines of the G-C base pairs are "flipped out" of the helix upon G-platination.[15] Duplex **I** offers the possibility for the competitive formation of both 3′–3′ 1,2–GG and a 5′–5′ 1,6–GG IXLs and we have previously shown (using 2D [^{1}H, ^{15}N] HSQC NMR spectroscopy) that Triplatin forms a 5′–5′ 1,6–GG IXL in the DNA duplex 5′–d{TATGTATACATA}$_2$ (duplex **II**).[5] Since duplex **I** offers the possibility for this cross-link to form, the minor product observed by ESI-MS in the study of its reaction with Triplatin[14] may indeed be the 1,6-cross-link formed as a result of rearrangement of the adducts under the experimental conditions. Herein we have used 1D ^{1}H and 2D [^{1}H, ^{15}N] HSQC NMR spectroscopy to follow the stepwise formation of interstrand cross-links by reaction of ^{15}N–Triplatin (^{15}N-**1**) with duplex **I** and to compare with the observed structural features of the isolated adduct.[14]

Experimental

Chemicals

The acetate salt of HPLC purified oligonucleotide 5′-{d(ACGTATACGT)$_2$} (duplex **I**) was purchased from GeneWorks (Australia). The nitrate salt of the fully ^{15}N labeled [*trans*-PtCl($^{15}NH_3$)$_2$}$_2$(μ-trans-Pt($^{15}NH_3$)$_2$($^{15}NH_2$-$(CH_2)_6$-$^{15}NH_2$)$_2$}]$^{4+}$ (^{15}N-**1**) was prepared according to previously reported procedures.[16]

NMR spectroscopy

NMR spectra were recorded on a Bruker AVANCE 600 MHz spectrometer (^{1}H, 599.92 MHz; ^{15}N, 60.79 MHz; ^{31}P, 242.94 MHz). The ^{1}H spectra were internally referenced to TSP and the ^{15}N chemical shifts externally referenced to $^{15}NH_4Cl$ (1.0 M in 1.0 M HCl in 5% D_2O in H_2O). The ^{1}H spectra were acquired with water suppression using the WATERGATE pulse sequence.[17] The 2D [^{1}H, ^{15}N] HSQC (heteronuclear single-quantum coherence) NMR spectra (decoupled by irradiation with the GARP-1 sequence during acquisition) optimized for $^1J(^{15}N,^1H)$ = 72 Hz were recorded using the standard Bruker phase sensitive HSQC pulse sequence.[18] ^{31}P spectra were referenced externally to phosphoric acid and acquired with a *zgig* pulse sequence. Typically for 1D ^{1}H spectra 32 transients were recorded with spectral width of 12 kHz and a relaxation delay of 1.5 s. For 2D [^{1}H, ^{15}N] HSQC NMR spectra 8 transients were collected for 128 increments of t_1 with an acquisition time 0.152 s and spectral widths of 2 kHz in f_2 (^{1}H) and 1.8 kHz in f_2 (^{15}N). 2D spectra were completed in 14 min and were processed using Gaussian weighting functions in both dimensions. For ^{31}P NMR spectra, 128 transients were recorded with a spectral width of 4.8 kHz, an acquisition time of 3.38 s and a relaxation delay of 0.25 s. 64 K data points were used for processing.

pH measurements

The pH of the solutions were measured using a Shindengen ISFET (semiconductor) pH meter (pH Boy-KS723 (SU-26F) and calibrated against buffers of pH 4.0 and 6.9. To avoid leaching of chloride ions, 5 μL samples were placed on the electrode and the pH recorded without returning the aliquot to the sample. Adjustments to the pH were carried out using 0.02, 0.05, 0.1 or 0.5 M solutions of either $HClO_4$ or NaOH in 5% D_2O/95% H_2O.

DNA preparation

Duplex **I** was desalted by means of a NAP-25 column and subsequently freeze-dried. This sample was dissolved in MilliQ H_2O (113 μL), then Na_3PO_4 buffer (30 μL, 150 mM, pH 5.6), $NaClO_4$ (90 μL, 0.5 M), D_2O (15 μL) and TSP (2 μL, 13.3 mM) were added to the NMR tube. To anneal the duplex, the sample was heated in a water bath to 90 °C and then allowed to cool to room temperature over a few hours. The concentration of duplex **I** was estimated by using UV spectrophotometry and ^{31}P NMR (relative to a known concentration of PO_4^3). A 2D ^{1}H NOESY NMRspectrum of the unplatinated duplex was recorded at 298 K and confirmed that the DNA had annealed properly.

Reaction of ^{15}N-1 and duplex I

A freshly made solution of ^{15}N-**1** was prepared by dissolving ^{15}N-**1** (0.41 mg, 0.33 μmol) in MilliQ H_2O (50 μL). In order to start the reaction, ^{15}N-**1** was added to the solution containing the annealed duplex **I** (preparation as described above). After accounting for dilution during adjustment of pH to 5.4, the final concentrations in the 300 μl sample volume were **1** (1.0 mm) and duplex **I** (1 mM) in 15 mM Na_3PO_4, 150 mM $NaClO_4$ in 5% D_2O. The reaction was followed by 1D ^{1}H and 2D [^{1}H, ^{15}N] HSQC NMR at 298 K to completion.

Data Analysis

Peak volumes in the Pt–$^{15}NH_3$ region of the 2D [^{1}H, ^{15}N] HSQC NMR spectra were measured using the plug-in '2D NMR Analysis' developed for ImageJ[19] and were then converted into concentrations relative to the initial concentration of ^{15}N-**1**. Changes in concentration were calculated by normalizing the percentage concentration of species observed per time point, after correcting for peak overlap, by the approach that we have described in detail elsewhere.[4, 5]

Results and Discussion

The reaction of ^{15}N-**1** with duplex **I** was followed using 2D [^{1}H, ^{15}N] HSQC and ^{1}H NMR spectroscopy. To allow for direct comparison with previous studies of the reaction of ^{15}N-**1** with other DNA sequences[4-6] similar conditions were chosen (pH 5.4, 298 K). The stepwise formation of the bifunctional lesion is illustrated in Scheme 1, showing the two possible GN7–GN7 interstrand cross-links that can be formed with duplex **I**: 3′–3′ 1,2–GG and 5′–5′ 1,6-GG. The ^{1}H and ^{15}N chemical shifts of all intermediate and bifunctional product species observed during the reaction are summarized in Table 1. Representative [^{1}H,^{15}N] HSQC NMR spectra are shown in Figure 1 and plots showing changes in the aromatic regions of the ^{1}H NMR spectra are shown in Figure 2.

Pre-covalent Binding Step.

The ^{1}H NMR resonances in the aromatic region of duplex **I** were assigned from 2D ^{1}H NOESY NMR data allowing for identification of specific changes that occurred immediately upon the addition of **1** to duplex **I** (Figure 3). The most notable changes occur for the H2 protons of A5 and A7 ($\Delta\delta$ = 0.08-0.1), consistent with pre-association of **1** in the minor groove of the duplex as we have observed previously in analogous reactions.[5] Minor shift changes ($\Delta\delta$ 0.02-0.04) occur also for the H8 protons of A5 and A7 and the H6 protons of C8, T6 and T10. From inspection of Figure 3, it appears that pre-association does not occur symmetrically along the duplex but more towards the 3′ end of **I**. It can be anticipated therefore that monofunctional binding to G9 will be preferred over binding to G9′ and binding to G3′ will be preferred over G3.

The pre-association is evident also in the 2D [^{1}H,^{15}N] HSQC NMR spectra recorded after addition of **1** to duplex **I** (Table 1 and Figure 1). The ^{1}H/^{15}N shifts of the terminal Pt–NH_3 groups (δ 3.90/–64.3) are identical to those seen for **1** in the presence of other sequences (e.g. **II** and **III**) where the ^{1}H resonances are slightly deshielded ($\delta\Delta$ = 0.04) compared to a sample of **1** in the absence of DNA, under identical conditions, consistent with H-bonding interactions between the Pt–$^{15}NH_3$ groups and the phosphate backbone of the DNA. The cross-peak corresponding to the {PtN_3O} end of the monoaqua monochloro species, **2** (δ 4.19/–61.6) has a similar pronounced downfield shift ($\Delta\delta$ ^{1}H = 0.19; ^{15}N 0.9) to the previous reactions, consistent with a stronger electrostatic interaction with the duplex than for **1**, as a consequence of the increased charge (+2). For the reactions with duplex **II** and **III** the linker Pt–NH_3 groups of **1** were strongly deshielded compared to the control sample, being most pronounced for duplex **II** ($\delta\Delta$ ^{1}H = 0.13;^{15}N = 0.9). A similar but slightly less pronounced deshielding effect is seen for the linker Pt–NH_3 groups in the presence of duplex **I** (see Table 1).

Monofunctional Binding Step.

Up to this point, the reaction of **1** and duplex **I** follows closely what has been previously observed: preassociation followed by aquation.[5] A characteristic feature of the platination of duplex **II** with **1**, as well as platination of duplex **III** with **1** and a variety of other PPCs,[4, 5, 12] is the observation of a single cross-peak (δ ~4.29/–61.0) corresponding to the Pt–$(NH_3)_2$ group bound to guanine N7 in the monofunctional adduct. This cross-peak is shifted significantly in both dimensions compared to the noncovalently bound compounds and is indicative of very similar H-bonded environments for the Pt–$(NH_3)_2$ groups in the different complexes, which are not influenced by differences in the polyamine linkers. In B form DNA the two ammines can form hydrogen bonds to guanine O6 and a phosphate oxygen atom.[4] The ^{1}H/^{15}N cross-peak for the Pt-$(NH_3)_2$ groups of the unbound {PtN_3Cl} end of the monofunctional adducts is typically slightly deshielded in the ^{1}H dimension ($\Delta\delta$ ^{1}H = 0.02) compared to the parent dichloro complex and is attributed to similar H-bonding interactions between the NH_3 groups of the unbound {PtN_3Cl} group and the DNA phosphate backbone.[4, 5, 12] In the present case while a single deshielded cross-peak is observed for the Pt-$(NH_3)_2$ groups of the unbound {PtN_3Cl} end of the monofunctional adduct(s) (δ 3.93/–64.2), after 1 h there are two distinct cross-peaks assignable to the monofunctionally bound Pt–$(NH_3)_2$ group (Figure 1, peaks **3a**). One (δ 4.27/–60.9) has a ^{1}H/^{15}N shift similar to that typically observed whilst the other (δ 4.22/–61.5) is significantly less deshielded in the ^{1}H dimension (by ~0.09 ppm). Based on the shift changes observed in the pre-association step (Figure 3) a reasonable intepretation is that monofunctional adducts are formed by binding to the non-equivalent G9 and G3′ residues. After approximately 1 h, two broadened resonances in the aromatic region of the ^{1}H NMR spectrum are observed at δ 8.54 and 8.46 ppm (Figure 2), consistent with platination of both G3′ and G9 ($\Delta\delta$ = 0.64 and 0.56, respectively). It is not possible to assign the Pt–NH_3 ^{1}H/^{15}N cross-peaks to the specific monofunctional adducts, or to calculate their relative intensity ratios, because as the reaction proceeds they become obscured by the product cross-peaks (Figure 1). That one of the ^{1}H/^{15}N cross-peaks is significantly less deshielded than typically observed suggests a difference in the H-bonding interactions between the Pt–NH_3 groups and the DNA, which could possibly occur if the approach to the guanine N7 is altered by anchoring of the linker group in the minor groove. For the Pt–NH_3 groups of the central linker a cross-peak is observed at δ 4.26/–63.6, which is slightly deshielded in the ^{1}H dimension compared to the pre-associated complex and has very similar ^{1}H/^{15}N shift to the monofuctional adducts formed by ^{15}N-**1** with duplex **II** and duplex **III** (see Table 1), indicating similar environments for these groups in each case. Notably two less intense and more strong deshielded peaks are observed (δ 4.31/–62.7, 4.28/–62.8; see Figure 1), which are assignable to the Pt–NH_3 groups in the central linker of a monofunctional adduct(s) based on their time dependent profiles. Overall these results suggest different structures for the monufuctional adducts. In one case the central {PtN_4} linker lies in an environment similar to that of the pre-associated complex in the minor groove, while the other has a different structure with more strongly H-bonded NH_3 groups.

Bifunctional Binding Step.

The monofunctional adducts formed by platination of either G9 or G3′ residues can transform into a 3′–3′ 1,2–GG IXL (G3′–G9), whereas the G3′-bound adduct can potentially form also a 5′–5′ 1,6–GG IXL (G3′–G3) (see Scheme 1). In our earlier study of the reaction of **1** and duplex **I**, significant formation of the 5′–5′ IXL was not observed, but instead the isolated adduct contained two simultaneous 3′–3′ 1,2–GG IXLs.[14] The [^{1}H,^{15}N] HSQC and ^{1}H NMR spectra provide evidence that both 3′–3′ and 5′–5′ IXLs are formed in the present case.

On completion of the reaction the aromatic region of the ^{1}H NMR spectra shows three resonances (with approximately equal intensities) at δ 8.58, 8.56 and 8.45, corresponding to the H8 resonance of platinated guanines in bifunctional cross-linked adducts (Figure 2). The 3′–3′ 1,2–GG IXL (in the sequence containing two covalently bound adducts) has two guanine H8 resonances at δ 8.53 (G3) and 8.41 (G9).[14] Based on these assignments the resonances at δ 8.58, 8.56 can both be assigned to platinated G3′, but in the distinct 3′–3′ and 5′–5′ IXLs, whereas the single peak at δ 8.45 is consistent with platinated G9 in the 3′–3′ IXL (noting the assumption above that monofunctional binding is to G9 and not to G9′). Based on this

assignment, and the relative intensities of the H8 resonances the ratio of 3′–3′ : 5′–5′ IXLs is *ca*. 2:1.

In the 2D [^{1}H, ^{15}N] HSQC spectra there is similar evidence for two distinct bifunctional IXLs. Two deshielded crosspeaks at δ 4.34/–61.1 and 4.31/–61.3 (labeled **4X** in Figure 1) are first visible after *ca*. 3 h and track together over the course of the reaction. They have similar ^{1}H/^{15}N shifts to a pair of peaks observed in the reaction of ^{15}N-**1** with duplex **III** (Table 1) and by analogy are assigned to two different $^{15}NH_3$ (end) groups coordinated to different Pt atoms of the same bifunctional adduct, which are H-bonded to guanine O6. In that case a broad peak at (δ 4.30/–60.9) was assigned to the other two Pt-NH_3 groups and a similar broad peak (δ 4.25/–61.3) is observed here. A ^{1}H/^{15}N cross-peak at δ 4.35/–63.3 also tracks with the two crosspeaks, **4X** and is assigned to the central Pt–$^{15}NH_3$ groups in the same bifunctional adduct. The ^{1}H/^{15}N cross-peaks for the second bifunctional adduct (labeled **4Y** in Figure 1) are strongly overlapped with those of the monofunctional adducts(s) and are only seen clearly when the reaction is complete. A sharp cross-peak assignable to the terminal Pt–NH_3 groups (δ 4.22/–61.6) is more shielded than for the other bifunctional adduct, or indeed for the bifunctional adducts of ^{15}N-**1** with duplex **II** and duplex **III**. Similarly, two sharp cross-peaks (δ 4.21/–63.9, 4.23/–63.3) and one broadened (δ 4.28/–63.5) cross-peak assignable to the Pt-NH_3 groups of the central linker are more shielded than observed previously. While it is not possible to make an unambiguous assignment, a reasonable interpretation is that **4X** is the 5′–5′ IXL (hence the Pt-NH_3 groups are in similar environments to the bifunctional adducts of **1** with duplex **II** and duplex **III**) and **4Y** is the 3′–3′ IXL. The previous study of the 3′–3′ 1,2–GG IXL showed that the platinum atoms coordinated in the major groove at N7 positions of guanine whist the central platinum unit is expected to lie in the DNA minor groove. The Pt–NH_3 groups of the central linker would therefore be expected to have similar ^{1}H/^{15}N shifts to those of the pre-associated complex, as is observed here.

Kinetics of Interstrand Cross-Link Formation.

In the previous studies of the reaction ^{15}N-**1** with duplex **II** and duplex **III** we were able to carry out a detailed kinetic analysis of the formation of the step-wise formation of the IXLs by monitoring the time dependent changes in the volumes of the ^{1}H/^{15}N cross-peaks for the Pt–$^{15}NH_3$ (end) groups in the 2D [^{1}H, ^{15}N] HSQC spectra. A similar analysis could not be carried out in the present case due to the greater degree of peak overlap; in particular the cross-peak for the {PtN_3O} group of the monoaquated species **2** becomes overlapped with those of the mono- and bifunctional adducts (see Figure 1). Figure 4 shows a time dependent plot of the relative concentrations of **1**, the combined monofunctional species (**3**) and total product (**4**), based on the relative intensity of the ^{1}H/^{15}N cross-peaks in the Pt–NH_3 (end) region, after making corrections for peak overlap. Comparison of the reaction profile with those reported previously,[5] suggests that the combined rate of monofuctional adduct formation occurs faster than for binding to duplexes **II** and **III**, whereas the combined bifunctional adduct formation occurs more slowly. In the present case the monofunctional species reach a maximum intensity of 55% of the total species in solution after *ca*. 10 h and although the reaction is mostly complete after 60 h, it takes a further 40 h for the combined bifunctional adducts to completely form. In contrast, for the reactions with duplexes **II** and **III**, the monofunctional species reaches a maximum intensity of ca 30% after 7 h and formation of the IXLs is complete within 45 – 48 h. [5]

Conclusions

Most DNA cross-linking agents bind predominantly in the 5′–5′ direction. There are few examples of cross-linking agents that do so in the antiparallel 3′–3′ direction. The results presented here provide evidence for the formation of both the possible 3′–3′ 1,2-IXL and the 5′–5′ 1,6-IXL, whereas in the previous reaction of **1** with duplex **I** the major adduct isolated by HPLC had two simultaneous 3′–3′ 1,2-IXLs.[14] The present study shows that the cross-link preference is kinetically controlled and will depend critically on the reaction conditions, in particular the **1**:duplex **I** ratio. If monofunctional binding occurs simultaneously at both G3 and G3′ then clearly formation of the 5′–5′ 1,6-IXL is ruled out, but two simultaneous 3′–3′ 1,2-IXLs can form. Some insight into cross-link formation preference may be obtained by considering that the rate of monofunctional binding to **I** (G3′ and/or G9) is faster than to duplex **II** (one unique G). This difference may be a reflection of the local environment and sequence context of the individual guanines. For example, in the reaction of 1,1/*t*,*t* with the 14-mer duplex 5′-d(ATACATG(7)G(8)TACATA)-3′.5′-d(TATG(25)TACCATG(18)TAT)-3′, monofunctional binding to the 3′G (G8) is at least sixfold faster than binding to the 5′G and no binding to the isolated Gs (18 and 25) was observed.[10] Overall the rates of closure of the combined bifunctional adducts are slower for **I** than for **II**. Previous NMR and molecular modelling studies of the reaction of **1** with duplex **II** showed that the "pre-associated" form in the *monofunctional* adduct must diffuse off the helix backbone prior to bifunctional adduct closure. This is inherently not necessary for the 3′–3′ adduct, as indicated by the structure of the adduct where the central platinum moiety is located in the minor groove.[14] Indeed, observation of very similar environments for the central NH_3 groups in **4Y** (assigned to the 3′–3′ IXL) with that of the pre-associated complex **1** is consistent with this interpretation.

The structure of the 3′–3′ 1,2-IXL shows little distortion apparent beyond the binding site.[14] This is in contrast to that of the 1,4-interstrand cross-link where the 5′–5′ IXL forms distinct conformers[5] and the structural distortions extend beyond the actual binding site.[20] In contrast, studies of the 3′–3′ 1,4-IXL with defined sequences showed severe distortion and multiple bifunctional adduct formation.[6] These features may have consequences for the details of repair of Pt-DNA adducts.[8, 9, 21-23] To mimic the interstrand crosslink of alkylating agents, Noll *et al.* constructed plasmid DNAs using modified cytosines incorporated into single CpG or GpC steps in small duplexes and then incorporated into plasmid DNA.[9] Both sequences were substrates for DNA repair enzymes but there is a four-fold difference in NER efficiency between the two, the CpG step being more robust. Interestingly, NMR structures of oligonucleotide decamers containing the CpG (5′–5′) IXL

showed a well-defined structure whereas the conformational disruptions of the CpG (3′–3′) precluded structural analysis by NMR.

The results again support the view that pre-association of the charged central linker in the minor groove dictates the directionality of cross-link formation and the plethora of structurally distinct cross-links formed by complexes such as Triplatin may be a significant factor in the the overall drug toxicity. It is axiomatic that multiple repair pathways will also exist in response to these diverse structures. Finally, searching for new platinum-based chemotypes has expanded significantly the description of ligand (Pt complex)-induced conformational changes of relevance to design of anti-cancer drugs.[24-26]

Acknowledgements

This work was supported by the Australian Research Council (Discovery grant to S.J.B-P and NF), National Institutes of Health (RO1-CA78754) and the University of Western Australia (University Postgraduate Award to RAR).

References

1. N. P. Farrell, *Drugs of the Future.*, 2012, in press.
2. J. B. Mangrum and N. P. Farrell, *Chem. Comm.*, 2010, **46**, 6640-6650.
3. V. Brabec, J. Kaspárková, O. Vrána, O. Nováková, J. W. Cox, Y. Qu and N. Farrell, *Biochemistry*, 1999, **38**, 6781-6790.
4. J. W. Cox, S. J. Berners-Price, M. S. Davies, Y. Qu and N. Farrell, *J. Am. Chem. Soc.*, 2001, **123**, 1316-1326.
5. A. Hegmans, S. J. Berners-Price, M. S. Davies, D. S. Thomas, A. S. Humphreys and N. Farrell, *J. Am. Chem. Soc.*, 2004, **126**, 2166-2180.
6. R. A. Ruhayel, J. J. Moniodis, X. Yang, J. Kasparkova, V. Brabec, S. J. Berners-Price and N. P. Farrell, *Chem.−Eur. J.*, 2009, **15**, 9365-9374.
7. J. Kasparkova, J. Zehnulova, N. Farrell and V. Brabec, *J. Biol. Chem.*, 2002, **277**, 48076-48086.
8. S. R. Rajski and R. M. Williams, *Chem. Rev.*, 1998, **98**, 2723-2796.
9. D. M. Noll, T. M. Mason and P. S. Miller, *Chem. Rev*., 2006, **106**, 277-301.
10. S. J. Berners-Price, M. S. Davies, J. W. Cox, D. S. Thomas and N. Farrell, *Chem. −Eur. J*., 2003, **9**, 713-725.
11. J. Zhang, D. S. Thomas, S. J. Berners-Price and N. Farrell, *Chem.−Eur. J*., 2008, **14**, 6391-6405.
12. R. A. Ruhayel, J. S. Langner, M.-J. Oke, I. Zgani, S. J. Berners-Price and N. P. Farrell, *J. Am. Chem. Soc*., 2012, **134**, 7135–7146.
13. J. Malina, N. P. Farrell and V. Brabec, *Chem.−Asian J.*, 2011, **6**, 1566-1574.
14. Y. Qu, M.-C. Tran and N. P. Farrell, *J. Biol. Inorg. Chem.*, 2009, **14**, 969-977.
15. H. Huang, L. Zhu, B. R. Reid, G. P. Drobny and P. B. Hopkins, *Science*, 1995, **270**, 1842-1845.
16. M. S. Davies, D. S. Thomas, A. Hegmans, S. J. Berners-Price and N. Farrell, *Inorg. Chem.*, 2002, **41**, 1101-1109.
17. M. Piotto, V. Saudek and V. Sklenar, *J. Biomol. NMR*, 1992, **2**, 661-665.
18. M. A. McCoy and L. Mueller, *J. Magn. Reson., Ser. A*, 1993, **101**, 122-130.
19. R. A. Ruhayel, B. Corry, C. Braun, D. S. Thomas, S. J. Berners Price and N. P. Farrell, *Inorg. Chem.*, 2010, **49**, 10815-10819.
20. Y. Qu, N. Scarsdale, M.-C. Tran and N. Farrell, *J. Biol. Inorg. Chem.*, 2003, **8**, 19-28.
21. L. Kelland, *Nature Rev. Cancer*, 2007, **7**, 573-584.
22. A. Sancar and J. T. Reardon, *Adv. Protein Chem.*, 2004, **69**, 43-71.
23. D. J. Stewart, *Crit. Rev. Oncol. Hematol.*, 2007, **63**, 12-31.
24. L. H. Hurley, *Nat. Rev. Cancer*, 2002, **2**, 188-200.
25. D. R. Boer, A. Canals and M. Coll, *J. Chem. Soc. Dalton Trans.*, 2009, 399-414.
26. V. Brabec and J. Kasparkova, *Drug Resist Updat.*, 2005, **8**, 131-146

Cite this: DOI: 10.1039/c0xx00000x

www.rsc.org/xxxxxx

ARTICLE TYPE

Table 1 $^{1}H/^{15}N$ chemical shifts for the Pt–$^{15}NH_3$ groups of ^{15}N-**1** and the intermediate species observed during the reaction with duplex **I** (at 298K, pH 5.4).[a] Data for the reaction of **1** with duplexes **II** and **III** under similar conditions are shown for comparison.[b]

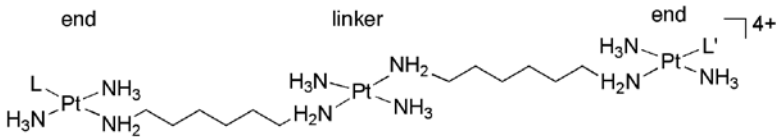

species	duplex **I**		duplex **II**[b]		duplex **III**[b]	
	Pt–$^{15}NH_3$		Pt–$^{15}NH_3$		Pt–$^{15}NH_3$	
L/L´	end	linker	end	linker	end	linker
	δ $^{1}H/^{15}N$	δ $^{1}H/^{15}N$	δ $^{1}H/^{15}N$	δ $^{1}H/^{15}N$	δ $^{1}H/^{15}N$	δ $^{1}H/^{15}N$
Cl/Cl	3.90/–64.3	4.24/–63.3	3.89/–64.4	4.28/–62.8	3.91/–64.2	4.27/–63.3
			(3.86/–64.4)[c]	(4.15/–63.7)[c]	(3.86/–64.4)[c]	(4.15/–63.7)[c]
Cl/H_2O	[d]	[d]	[d]	[d]	[d]	[d]
Cl/H_2O	4.19/–61.6		4.15/–61.9		4.19/–61.8	
			(4.00/–62.5)[c]		(4.00/–62.5)[c]	
Cl/GN_7	3.93/–64.2	4.26/–63.6	3.93/–64.3	4.27/–63.7	3.93/–64.2	4.28-4.29/–63.3
Cl/GN_7	4.22/–61.5		4.31/–61.1		4.29/–60.6	
	4.27/–60.9					
GN_7/GN_7						
5´–5´	4.34/–61.1[f]	4.35/–63.3	4.37/–61.0	4.40/–63.1	4.37/–60.6[f]	4.29/–63.5
	4.31/–61.3[f]		4.31/–61.1[e]	4.31/–63.6	4.35/–60.9[f]	
	4.25/-61.3[e,g]			4.28/–63.6	4.30/–60.9[e]	
3´–3´	4.22/–61.6	4.28/–63.5[e,g]				
		4.23/–63.3				
		4.21/-63.9				

[a] ^{1}H referenced to TSP (internal) and ^{15}N referenced to $^{15}NH_4Cl$ (external). δ in ^{15}N dimension ± 0.2 ppm. [b] From reference [5]; conditions are not stictly comparable as the sample of duplex **I** in this work contains 150 mM $NaClO_4$ in addition to 15mM Na phosphate. In the case of duplex **III**, two conformers of the 1,4 5´–5´ IXL were observed; only cross-peaks for the major conformer are listed here for clarity. [c] The $^{1}H/^{15}N$ chemical shifts in the absence of DNA at pH 5.4. [d] Assumed to be concealed underneath the cross-peak corresponding to the Cl/Cl species. [e] Broad peak. [f] Pair of peaks. [g] Both the 5´–5´ and 3´–3´ IXLs may contribute to this cross-peak.

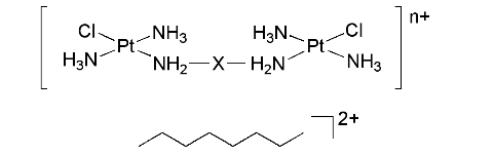

1,1/*t,t* (BBR3005)

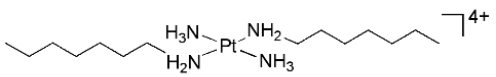

1,0,1/*t,t,t* (Triplatin, BBR3464, 1)

5'-ACGTATACGT-3' 3'-TGCATATGCA-5'	duplex **I**
5'-TATGTATACATA-3' 3'-ATACATATGTAT-5'	duplex **II**
5'-ATATGTACATAT-3' 3'-TATACATGTATA-5'	duplex **III**

Chart 1

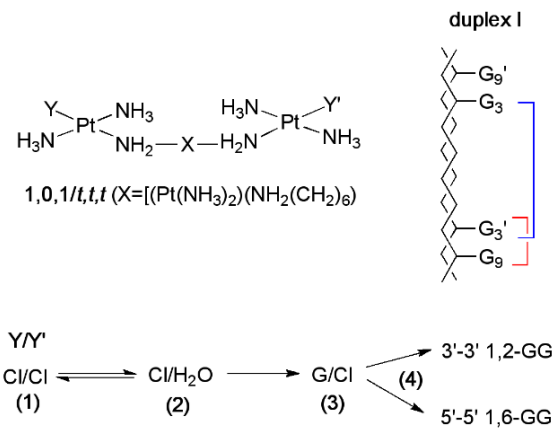

Scheme 1. Reaction of ^{15}N-**1** with duplex **I**. The two possible GN_7–GN_7 interstrand cross-links are labelled: 3´–3´ 1,2–GG IXL (red) and 5´–5´ 1,6-GG IXL (blue).

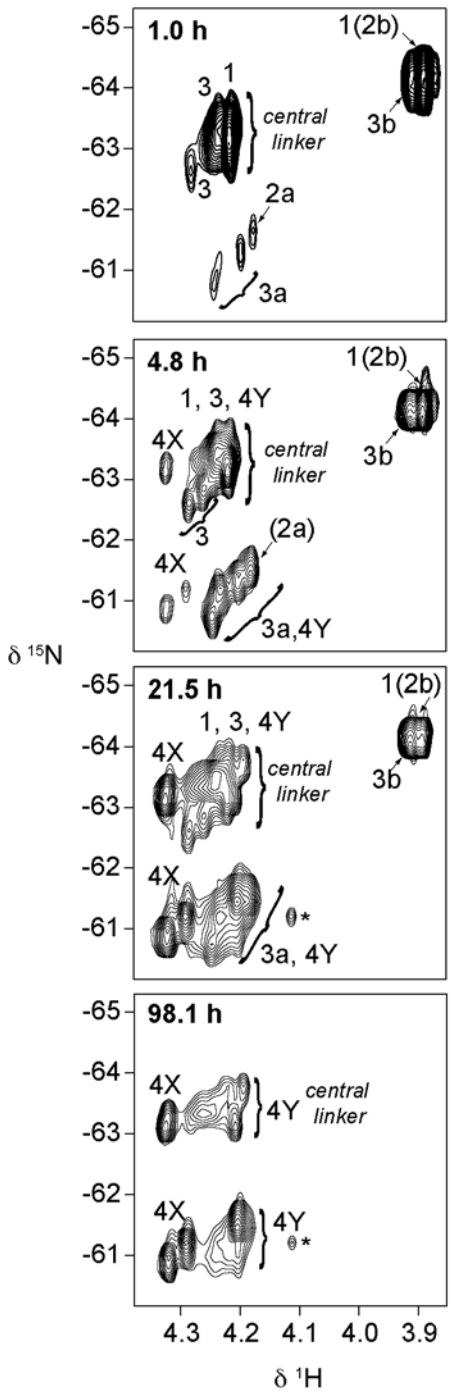

Figure 1. 2D [^{1}H,^{15}N] HSQC NMR (600 MHz) spectra recorded at 298K of ^{15}N-**1** after addition to duplex **I** for the times shown. Peaks have been assigned to the end and linker Pt–$^{15}NH_3$ groups for the structures **1**–**4** shown in Scheme 1. The peak labelled '*' is assigned to a phosphate derivative {PtN_3OP} of ^{15}N-**1** based on species observed previously.[16]

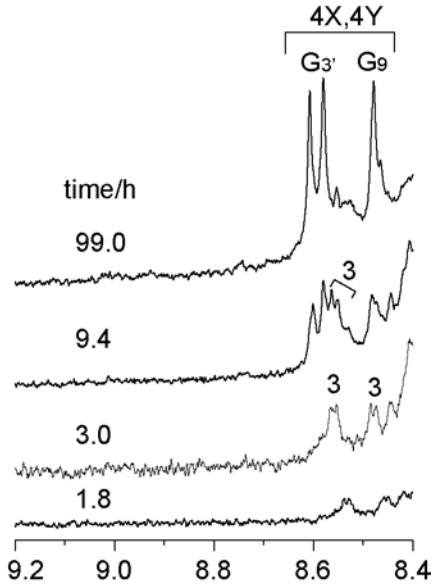

Figure 2. The aromatic region of the ^{1}H NMR spectra (600 MHz) of duplex **I** after the addition of ^{15}N-**1** for the times shown. Assignments have been made for the monofunctional species (**3**) and the bifunctional adducts (**4X** and **4Y**).

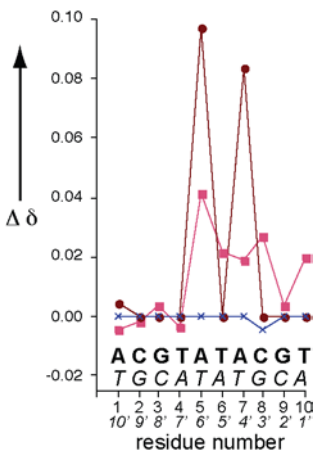

Figure 3. ^{1}H chemical shift changes ($\Delta\delta = \delta$ (duplex **I**: ^{15}N-**1**) - δ (duplex **I**)) seen after the addition of ^{15}N-**1** to duplex **I**. Key: circles (brown) H2 protons; squares (red) aromatic H8/H6 protons; × (blue) H41 protons. The complementary strand is shown in italics.

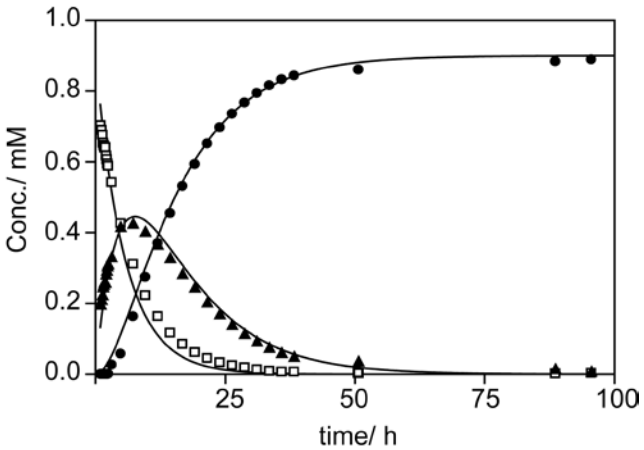

Figure 4. Plots of the relative concentrations of species observed during the reaction of ^{15}N-**1** with duplex **I,** based on intensities of the cross-peaks in the Pt-$^{15}NH_3$ region of the 2D [^{1}H, ^{15}N] HSQC spectra. Labels: dichloro species (**1**) open squares; monofunctional species (**3**) filled triangles; bifunctional adducts (**4**) filled circles.